aerodynamic shape, specifically in reference to the large wetted area associated with the fuselage and its consequent tapering around the wing root to lessen the adverse pressure gradients which may occur otherwise.

COMSOL was used to model the fluid flow around these particular parts. As a follow-on study, structural parameters were input and the mechanical behavior of the airframe then observed simultaneously. Additionally, we explored the flow field around a two-dimensional airfoil section and the effect of heat generation related to the solar cells.

2. Problem Formulation

The primary objective of winglets is to reduce overall drag. Originally, endplates were seen as a way to curb induced drag on real wings but it wasn't until much later that winglets came into the form that we can all appreciate today on modern airliners [15]. There are various schools of thought in wingtip device design and some devices try to merge these ideas. Planar devices usually try to either capture the strength of the trailing vortices or delay their creation further outboard. Non-planar devices usually aim to do the same but tend to be more efficient since they are out of the wing's plane.

Winglets have become an economical way of retrofitting existing aircraft with a modification that lessens induced drag and thus reduces the power requirements to fly at a particular airspeed. In the late 1980's and early 1990's, many would argue that winglets require too much design work to be effective, especially at slower speeds [11]. This was in part due to the lack of computing power and the difficulty involved in optimizing these non-planar lifting surfaces for more than one flight condition. Similarly, a balance must be found between the reduction in induced drag and the increase in parasitic drag that incurs with respect to the new wetted surfaces. For a further discussion on induced and parasitic drag, please consult [6] and [14].

Winglets conventionally have a set of geometric parameters which can be modified to achieve desired performance. In addition to these parameters, the airfoil used for a winglet will usually differ from the wing's airfoil selection since it effectively is implemented for a different purpose. For a more detailed discussion on these various parameters and how they may affect the results, refer to [8].

The goal of this part of the study was to minimize the drag of the overall plane in all flight conditions. Due to the size restrictions put upon the project, the aspect ratio achieved was not nearly as high as other contemporary solar airplanes. To combat this heightened induced drag factor and to better span efficiency, the incorporation of winglets are studied and developed.

Additionally, winglets usually increase wing bending moment, especially if they result in a wingspan increase or if they are non-planar lifting surfaces. As a result, a structural study had to be completed to ensure that the desired fabrication techniques and material selections were still appropriate.

On an already highly optimized aerodynamic body, one of the major drag penalties arise from junction flow, categorized as interference drag [11]. Junction flows are highly proprietary in that they cannot be generalized. Every situation is simply different, and while broad guidelines may be outlined, seldom will they be the complete answer. For further discussion on juncture flows and three-dimensional boundary layer interaction, see [12].

Composites have made complex, aerodynamically advantageous shapes a reality. As with winglets, increasing computing power and more accurate fluid flow models have ramped up interest in the analysis and design of wing-fuselage flow interaction. See [9] and [5], for example.

The main objective of this part of the study was to minimize flow separation, which occurs at the junction and thus lessen the overall drag of the plane. Additionally, the overall fuselage design was modeled to view the flow field and pressure distribution to ensure that laminar flow was preserved. One major design criterion of the fuselage is to minimize and separate the adverse pressure gradients. Another vital evaluation criterion is the interaction of the streamlines from the upper and lower halves of the fuselage, as well as the trailing edge of the wing. This evaluation is even further complicated, and generally dictated by, the taper of the fuselage around the airfoil section.

Finally, a side study concerning the fluid flow over a solar-cell coated airfoil section is presented. In this on-going study, the flow field is analyzed for changes over the airfoil section as all three heat transfer modes are active. This model is currently being built up to accept a wider range of inputs, as discussed in the next section.

3. Models and Resources

As most problems involved with fluid flow, a setup that would constitute a virtual wind tunnel was ideal. All of the three-dimensional problems could be divided along the longitudinal axis for symmetry. After the models were imported from the SolidWorks, a box was created which surrounded the whole of the model and gave sufficient room around the object to analyze the flow, yet was tight enough to lower the number of internal nodes to a minimum. Figure 1 illustrates such a configuration for a wing-junction flow study.

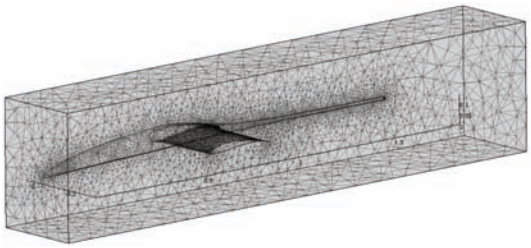

Figure 1. Wing-junction flow model, isometric view.

Typically, the fluid box was modeled to have one inlet and one outlet, three slip surfaces and one symmetry boundary, at the root of the geometry being analyzed. The geometry itself consisted of non-slip interior boundaries. The box also provided easy boundary specifications for the structural problems. Additionally, this method allowed easy estimation of the drag forces produced by the various components, if desired.

Most models had around 170,000 elements, depending on the physical size of the object being studied and the accuracy desired. A mesh this size yielded about 580,000 degrees of freedom, on average, for a single physics problem.

COMSOL's built-in fluid dynamics package uses the Navier-Stokes equations, as shown in (1) and (2).

$$\frac{\partial \vec{V}}{\partial t} + \vec{V} \cdot \nabla \vec{V} = -\nabla p + \mu \nabla^2 \vec{V} \qquad (1)$$

$$\frac{\partial T}{\partial t} + \vec{V} \cdot \nabla T = \nabla \cdot (k \nabla T) + S \qquad (2)$$

Various solvers were used for the fluid flow problems but generally speaking GMRES and FGMRES gave the best results when paired with Geometric Multigrid preconditioning. The pre- and postsmoothers played a large role in COMSOL's ability to converge, but for the flow analysis the Vanka algorithm worked well. Additionally, COMSOL's adaptive solver was used in conjunction with these settings with good results. Some issues related to these choices will be discussed later.

For the structural analysis, the multiphysics aspect of the problem and the desire to simultaneously solve the fluid and structure problem proved demanding, but COMSOL's fluid-structure interaction module handled these problems properly and efficiently with the default segregated solver settings, with minor modifications to the geometric multigrid solver. The fluid-structure module employs the previously mentioned Navier Stokes equations coupled with a solid stress-strain physics module and a moving mesh module (ALE method). COMSOL's free mesh utility had trouble dealing with some of the structure's areas with more curvature and an automatic mesh hierarchy could not be readily achieved. This was resolved by building specific mesh cases but computing times were found to be quite sluggish for some of the geometries.

For the two-dimensional multiphysics problem involving flow and heat transfer, a similar arrangement to the three-dimensional problems was used with a fluid box being built around the airfoil. The fluid-thermal module was used for this problem. For the fluid sub-problem, there is one inlet, one outlet and two slip surfaces, with the airfoil's surface set as a non-slip interior boundary. The Weakly Compressible Navier Stokes mode was employed since the fluid's density is expected to change, although slightly, with pressure and temperature. For the heat transfer, the boundaries were slightly more complicated. Figure 2 illustrates the problem configuration.

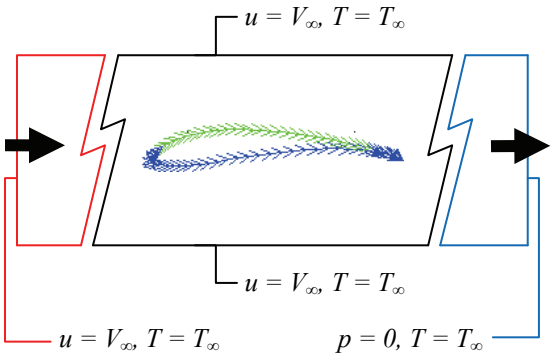

Figure 2. Boundary layout, heat generation module.

The airfoil's top surface, highlighted in green in Figure 2, is considered a heat source to mimic an embedded thin-film solar panel. This surface also produces radiation that is both surface-to-ambient and surface-to-surface. The conduction through the panel itself is ignored since it is 60 microns thick. The energy emanating from the panel can be described as a function of its efficiency and the solar flux, as in equation (3), where q_0 denotes the heat generated, η is the solar panel efficiency and I is the solar intensity, in units of W/m^2.

$$q_0 = (1 - \eta)I \tag{3}$$

The panel section of the airfoil can be formulated as a heat generator. Additionally, η varies with temperature T, in degrees Kelvin, as described by equation (4). This equation was determined by gathering empirical data from solar cells used in a past iteration of the UAV project. The model could be made to consider a variety of solar panels but this not within the scope of this study. The final term in the equation represents peak cell efficiency. For example, these particular cells have a maximum efficiency of 5% while more efficient cells may run as high as 10 to 15%.

$$\eta = \frac{-(T^2 - 303.5)^2}{10^5} + 0.05 \tag{4}$$

The bottom surface of the airfoil, which can be viewed as the remainder of the airfoil boundary in black on Figure 2, is modeled as continuity, or equation (5). The edges of the fluid box, the box around the airfoil, have temperature boundaries, as prescribed by equation (6). This simulates an ambient temperature envelope.

$$\sum(-n[-k\nabla T]) = \varepsilon\sigma(\Delta T^4) \tag{5}$$

$$T = T_0 \tag{6}$$

The temperature of the airfoil core starts at an initial temperature which matches the sub-domain's initial temperature. With the model generated in such a way, solar radiation is assumed to be constant. The model could be built to further consider additional variables.

A dedicated machine was built to solve these problems. Using previous experience with the COMSOL engine, requirements for a simulation workstation were put together. An abbreviated components list can be viewed in Table 1. The final cost, as of August 2008, was around $1,300 USD. Table 2 outlines some of the results used to benchmark the machine's speed and stability.

4. Results

COMSOL's output capabilities allowed us to easily and quickly analyze the results from simulations and gather a tremendous amount of information simply by inspection. Figure 3 shows how isosurface plots of the flow over the fuselage were used to determine where and how pressure gradients occurred, and how to move through the design iterations to properly optimize the shape.

While the primary function of the fuselage is to carry avionics and payload, the adverse pressure gradients near the wing must be minimized to reduce drag and special thought

Table 1: Workstation components list.

CPU	Intel Q9450 Quad Core, rated at 2.66GHz per core, operating at 3.2GHz per core
RAM	PC8500 RAM, 8GB, tightened timings 3-3-3-14, operating at 866MHz
Chipset	Intel P43
Video	Nvidia 9600GT
OS	Microsoft Vista Enterprise 64-bit

Table 2: Workstation benchmarking; free bi/tri-linear mesh; GMRES, Geometric Multigrid except 04 (PARDISO).

Benchmark Model Name	Analysis Type	Number of Elements	Number of Degrees of Freedom	Time to Solution (seconds)
01	Fluid, Steady State, 3D	56,780	261,567	1209.12
02	Fluid, Steady State, 3D	157,570	651,248	3345.67
03	Fluid, Steady State, Adaptive, 3D	9361/31096	45043/140756	8584.35
04	Fluid-Thermal Interaction, 2D	3433	21191	37.64
05	Fluid-Structure Interaction, 3D	4078	37299	377.03

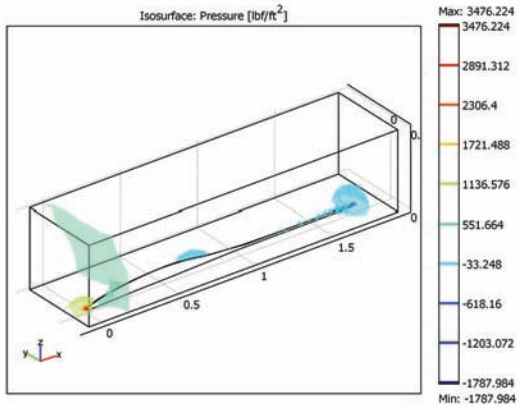

Figure 3. Isosurface plot of the pressure distribution (lb_f/ft^2) around the fuselage.

must be put into its shaping. A secondary objective is to keep the flow laminar over the body of the plane for as long as possible and to prevent separation in areas with complex boundary layer interaction; for example, at the wing-fuselage junction. Figure 4 shows a close-up of such a junction flow study. According to [9], only 20% of the wingspan from the root need be included to obtain valid results.

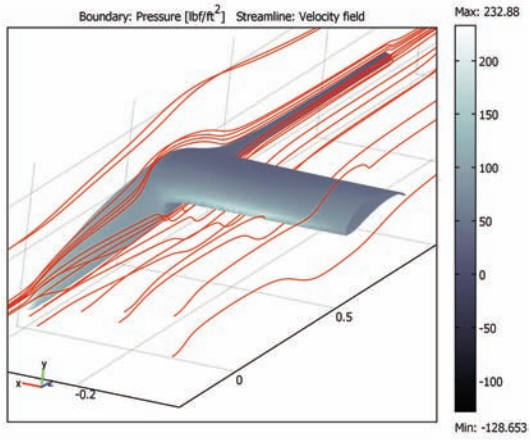

Figure 4. Fluid flow at the wing-fuselage junction, with surface pressure (lb_f/ft^2) and velocity streamlines.

The winglet design study has so far shown an overall drag reduction of 8.1% at cruise condition over the original wing design, with smaller reductions in other flight conditions, such as turning flight or landing approach. Superimposition of the gathered data from COMSOL onto the UAV's flight polars shows no performance penalties. Figure 5 outlines the typically sought information from COMSOL, such as isosurface pressure plotting, velocity and vorticity streamline fields and boundary velocity plots, among others. Figure 6 compares pressure and flow behavior over the original wing and one of the winglet design iterations.

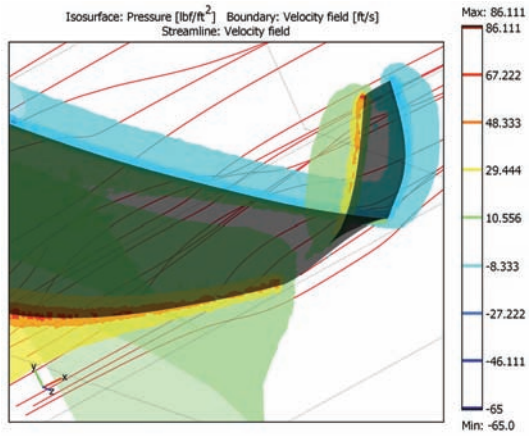

Figure 5. Typical COMSOL output for winglet study: isosurface pressure distribution (lb_f/ft^2) and velocity streamlines.

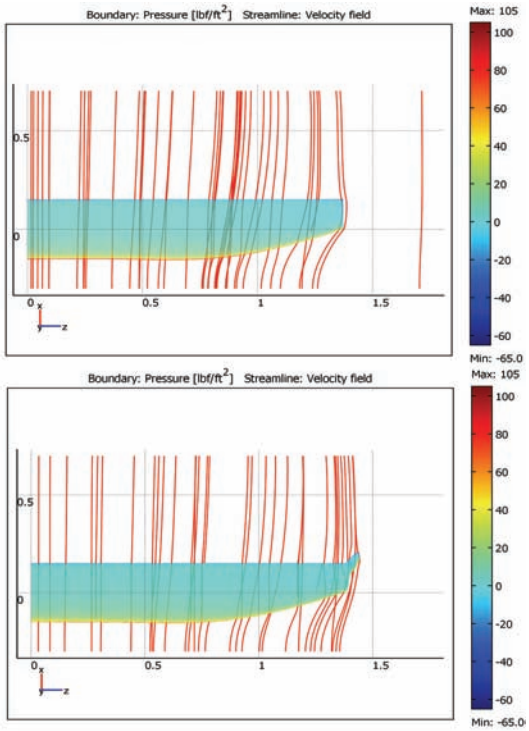

Figure 6. Flow field comparison between original wing and winglet design (top and bottom). Depicted: boundary plots representing surface pressure (lb_f/ft^2) and velocity streamlines.

COMSOL's boundary integration mode is especially powerful when coupled with the weak

constraint variables. The boundary integration mode itself allows us to quickly find changes in overall drag. The weak constraint variables offer an easy way of computing the coefficients of drag and lift, if desired. This feature was used in numerous instances during the fluid flow analysis, both as a way to benchmark the accuracy of the models against known values and the obtained results against predicted data using various panel methods.

The fluid-structure analysis allowed us to dynamically observe the effect of the incorporation of winglets on the airframe, both from an aerodynamics and structural point-of-view. The results could be numerically compared to the original cases and direct considerations regarding the manufacturing of the airframe could be completed on the fly. For example, using one of the evaluated building materials, polystyrene, the original wing showed a deflection of 0.0004" at the tip, as compared to a 0.007" tip deflection with a winglet device. Figure 7 shows typical output in close-up.

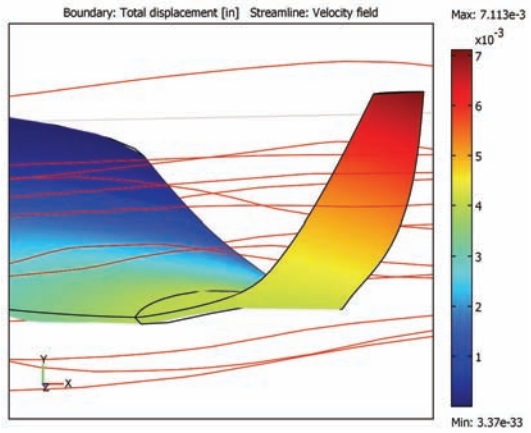

Figure 7. Boundary plot showing wing total displacement (in) with velocity streamlines.

Additional data regarding the complete airframe was gathered by studying the flow field around the complete structure. Such simulations enabled a direct correlation between estimated flight polars from the original sizing study and COMSOL's numerically evaluated aerodynamic values, such as the various lift and drag coefficients earlier discussed. In general, the data agreed well. Additionally, estimated values from the sizing study, such as overall zero-lift drag coefficient, could now be validated numerically and flight performance could be assessed at a deeper level. Figure 8 shows one such simulation's output.

The fluid-thermal analysis on the two-dimensional airfoil section is still on-going but preliminary results have been obtained and the study is being pushed ahead toward more ambitious concepts. So far, COMSOL's multiphysics abilities have been used to observe the effect of heat generation on the flow and its propagation through the wing core, through a simplified model as described earlier. Figure 9 shows a surface plot of the temperature profile around and in the airfoil section, coupled with a streamline plot.

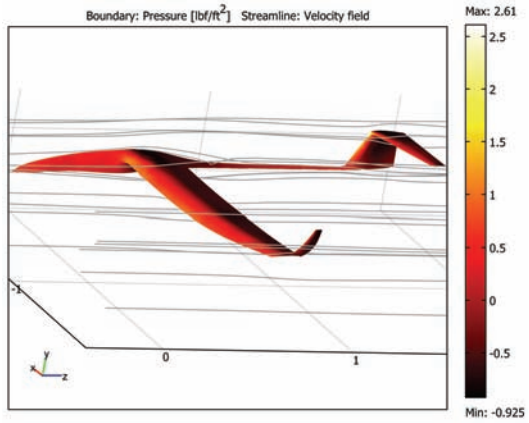

Figure 8. Full airframe fluid analysis with boundary plot showing surface pressure (lb_f/ft^2) and velocity streamlines for flow analysis.

These plots revealed some interesting information which was not expected at the onset of the study. For example, the maximum service temperature of some of the building materials in the wing core were quite low and it was found that this temperature could be exceeded in some cases.

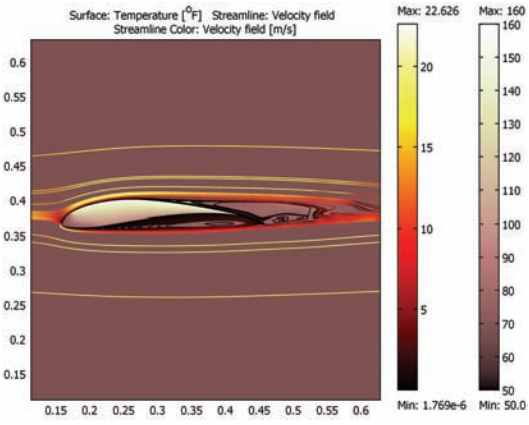

Figure 9. Heat propagation in the flow field (surface plot, ºF) plotted with velocity streamlines (m/s).

5. Conclusion

COMSOL Multiphysics 3.4 proved to be a valuable tool in the development of the UNLV solar-powered UAV. In overview, we have demonstrated that this software package can be used for small-scale evaluation of flying platforms, such as UAVs, and that the multiphysics package provides an all-inclusive way to approach a design problem and quickly come up with a development solution.

COMSOL provided results in a timely manner and allowed the designers of the UAV to optimize key parts of the airframe, primarily from an aerodynamics standpoint, but also to observe the structural side effects of these modifications. The ability to simulate various flight conditions using single or multiple physics enabled the iterative design process and facilitated the development of the design into a (numerically) ready airframe. The fluid and structure modules were effective but COMSOL's mesher had difficulties with the complex curvature of the airfoil profile and its subsequent extrusion along the wing's span. This issue may have also resided partially with the CAD import module. These two issues resulted in dramatic increases in preparation time for some of the simulations.

Additionally, it was shown that COMSOL can be run on a high-end desktop personal computing machine to provide accurate results in respectable computing times for fairly complex problems. It was found on this machine that, using the GMRES solver, meshes with up to two million degrees of freedom could be solved before running out of memory.

6. References

[1] AC Propulsion. (2006, February 2). *Technology - SoLong UAV*. Retrieved August 10, 2007, from http://www.acpropulsion.com/solong/

[2] Boermans, L. (2006). *Research on sailplane aerodynamics at Delft University of Technology. Recent and present developments.* Presentation, Delft University of Technology, Delft.

[3] Boermans, L., Kubrynski, K., & Nicolosi, F. (1997). Wing-Fuselage Design of High-Performance Sailplanes. In R. Henkes, & P. Bakker (Ed.), *Boundary-Layer Separation in Aircraft Aerodynamics* (pp. 23-41). Delft: Delft University Press.

[4] Brandt, S. A., & Gilliam, F. T. (1995). Design Analysis Methodology for Solar-Powered Aircraft. *Journal of Aircraft , 32* (4), 703-709.

[5] Green, B. E., & Whitesides, J. L. (2003, March-April). Method for Designing Leading-Edge Fillets to Eliminate Flow Separation. *Journal of Aircraft , 40* (2), pp. 282-289.

[6] Kuethe, A. M., & Chow, C.-Y. (1986). *Foundations of Aerodynamics* (Fourth Edition ed.). New York: John Wiley & Sons.

[7] Maughmer, M. D. (2002, June). About Winglets. *Soaring Magazine* .

[8] Maughmer, M. D. (2003). Design of Winglets for High-Performance Sailplanes. *Journal of Aircraft , 40* (6), 1099-1106

[9] Maughmer, M., Hallman, D., Ruszkowski, R., Chappel, G., & Waitz, I. (1989, August). Experimental Investigation of Wing/Fuselage Integration Geometries. *Journal of Aircraft , 26* (8), pp. 705-711.

[10] Noth, A. (2008). *History of Solar flight.* Electronic Report, Swiss Federal Institute of Technology Zürich, Autonomous Systems Lab, Zürich.

[11] Raymer, D. P. (1999). *Aircraft Design: A Conceptual Approach* (Third Edition ed.). Reston, Virginia, United States of America: American Institute of Aeronautics and Astronautics, Inc.

[12] Schlichting, H., & Gersten, K. (1999). *Boundary Layer Theory* (8th Revised and Enlarged Edition ed.). (K. Mayes, Trans.) New York: Springer.

[13] Thomas, F. (1999). *Fundamentals of Sailplane Design.* (J. Milgram, Trans.) College Park, Maryland: College Park Press.

[14] Thwaites, B. (1960). *Incompressible Aerodynamics.* New York: Oxford University Press.

[15] Whitcomb, R. T. (1976). *A Design Approach and Selected Wind-Tunnel Results at High Subsonic Speeds for Wing-Tip Mounted Winglets.* NASA, Langley Research Center. Hampton: NASA.